

# On the Structure of the Hoyle State in $^{12}\text{C}$

M. Chernykh,<sup>1</sup> H. Feldmeier,<sup>2</sup> T. Neff,<sup>3</sup> P. von Neumann-Cosel,<sup>1</sup> and A. Richter<sup>1</sup>

<sup>1</sup>*Institut für Kernphysik, Technische Universität Darmstadt, D-64289 Darmstadt, Germany*

<sup>2</sup>*Gesellschaft für Schwerionenforschung, D-64291 Darmstadt, Germany*

<sup>3</sup>*National Superconducting Cyclotron Laboratory, Michigan State University, East Lansing, MI 48824, USA*

(Dated: September 11, 2006)

The first excited  $0^+$  state in  $^{12}\text{C}$  (Hoyle state) has been predicted to be a dilute self-bound gas of bosonic  $\alpha$ -particles, similar to a Bose-Einstein condensate. In order to clarify this conjecture precise electron scattering data on form factors of the ground state and the transition to the Hoyle state are presented and compared with results of the Fermionic Molecular Dynamics model, a microscopic  $\alpha$ -cluster model and an  $\alpha$ -cluster model with reduced degrees of freedom (in the spirit of a Bose-Einstein condensed state). The data indicate clearly a dilute density with large spatial extension for the Hoyle state. A closer inspection of the model calculations, which reproduce the experimental findings, reveals that the term Bose-Einstein condensation of three  $\alpha$ -particles must not be taken too literally.

PACS numbers: 25.30.Dh, 21.10.Dr, 21.60.Gx, 27.20.Gn

The production of the element carbon is a key reaction of stellar nucleosynthesis. Its most abundant isotope,  $^{12}\text{C}$ , is created in the fusion of three  $\alpha$  particles through the formation of the short-lived  $^8\text{Be}$  ground state as intermediate state [1]. Early on, Hoyle recognized that the observed abundance requires an accelerating mechanism and he postulated [2] the existence of a  $J^\pi = 0^+$  excited state in  $^{12}\text{C}$  close to the threshold for  $^8\text{Be} + ^4\text{He}$  fusion. Indeed, such a state at an excitation energy  $E^* = 7.654$  MeV in  $^{12}\text{C}$  was experimentally confirmed soon afterwards [3]. Despite its astrophysical relevance, to date the production rate through the above mechanism is known with insufficient precision only [4, 5].

In nuclear structure this so-called ‘Hoyle state’ is playing a prominent role as a prototype of  $\alpha$ -cluster states in light nuclei. Unlike the ground state its description poses a continuing challenge to shell model approaches. Even the most advanced no-core calculations using very large model spaces fail [6]. In fact, this state is not tangible in models using a harmonic oscillator basis. On the other hand, cluster models have been popular for describing the spectrum of  $^{12}\text{C}$  (for some recent work see e.g. [7–10]). Recently it has been pointed out that the Hoyle state can be viewed as a dilute gas of weakly interacting  $\alpha$  particles resembling the properties of a BEC [11–16].

The purpose of this letter is to investigate the structure of the Hoyle state with experimental data on electron scattering which is the ideal method to map the charge distribution of nuclei. Extensive data up to high momentum transfers  $q \approx 3 \text{ fm}^{-1}$  exist for elastic electron scattering on  $^{12}\text{C}$  (see [17] and references therein) as well as for the transition to the Hoyle state [18] including some recent measurements [19] at the superconducting Darmstadt electron linear accelerator S-DALINAC extending previous data at low  $q$  [20]. The most appropriate experiment would be a study of elastic electron scattering on the Hoyle state itself which, however, is impossible

because of its short lifetime. Instead one has to revert to the available data summarized above.

These data are then compared with the predictions of different theoretical models. The first model is the Fermionic Molecular Dynamics (FMD) approach [21] which spans the many-body Hilbert space with Slater determinants built on single-particle wave packets of Gaussian shape. To recover the symmetries of the Hamiltonian the intrinsic Slater determinants are projected on angular and total linear momentum. The effective nucleon-nucleon interaction  $V_{\text{UCOM}}$  employed here is derived from the realistic Argonne V18 potential by means of the Unitary Correlation Operator Method (UCOM) [22] which explicitly treats the effects of short-ranged repulsive and tensor correlations. It is augmented with a phenomenological correction (total strength about 15% of  $V_{\text{UCOM}}$ ) adjusted to reproduce the binding energies of  $^4\text{He}$ ,  $^{16}\text{O}$ ,  $^{40}\text{Ca}$ ,  $^{24}\text{O}$ ,  $^{34}\text{Si}$  and  $^{48}\text{Ca}$  as well as the charge radii of  $^4\text{He}$ ,  $^{16}\text{O}$  and  $^{40}\text{Ca}$ . This model reproduces many features of nuclei up to mass number  $A \approx 60$ .

The variational parameters of the FMD wave functions are the parameters of the single-particle states. The FMD states are very flexible and can describe cluster states as well as shell-model like configurations. In the present calculation the many-body basis consists of 16 intrinsic states obtained in a variation after angular momentum projection procedure (projecting on  $0^+$  and  $2^+$  states) with constraints on the radii and additional 57 states that have been iteratively selected to minimize the energies of the first three  $0^+$  states. These states are chosen out of a set of 42 FMD states obtained in variation after parity projection with constraints on radii and quadrupole deformation and 165 explicit  $\alpha$ -cluster triangle configurations. An  $\alpha$  cluster is defined here as a product of four Gaussian single-particle states with total spin and isospin equal to zero. The Antisymmetrized Molecular Dynamics (AMD) model (see [23] for a recent dis-

cussion of  $^{12}\text{C}$ ) uses similar wave functions but imposes a fixed width parameter for the Gaussian wave packets. As shell-model like states and cluster states prefer different widths in  $^{12}\text{C}$  this is an important downside when compared to the FMD approach.

In a second model (labeled  $\alpha$ -cluster) we restrict ourselves to the  $\alpha$ -cluster triangle configurations. Convergence for the first three  $0^+$  states is achieved with a subset of 55 states. In this case we essentially implement a microscopic  $\alpha$ -cluster model using Brink-type [24] wave functions. However, with the  $\alpha$ -cluster states alone a significant underbinding is observed when the FMD Hamiltonian is used. Therefore, we employ the modified Volkov V2 interaction proposed in [25] which is fine-tuned to reproduce the ground and Hoyle state energies in  $^{12}\text{C}$  within an  $\alpha$ -cluster model. One has to keep in mind that this interaction is especially tailored and can not be used in other nuclei, for example for  $^{16}\text{O}$  it already leads to an overbinding of about 25 MeV. The addition of a spin-orbit force would destroy the reproduction of the  $^{12}\text{C}$  ground state properties. Therefore the predictive power is limited.

The same interaction is used in the third model (labeled ‘BEC’) by Funaki *et al.* [12]. Here the number of degrees of freedom is reduced even further by using basis states where the center-of-mass coordinates of all the  $\alpha$ -clusters are given by the same (deformed) wave function like in a Bose-Einstein condensate. Of course the state has to be antisymmetrized finally. The bosonic nature of the wave function therefore only survives when the density of the  $\alpha$  clusters is low enough such that antisymmetrization is not important. This is certainly not the case for the ground state and only to a certain extent for the Hoyle state. A detailed analysis [26] within an  $\alpha$ -cluster model, using a slightly different interaction, shows that the probability to find all  $\alpha$  clusters in the same  $S$ -wave orbit is about 30% for the ground state and about 70% for the Hoyle state. Thus the attribute ‘Bose-Einstein condensate’ should not be taken too literally.

A comparison of the three models for energies, radii and transition strengths in  $^{12}\text{C}$  is shown in Table I. The  $\alpha$ -cluster results agree very well with the ‘BEC’ approach and also with resonating group method (RGM) calculations [25]. All models give very large radii for the Hoyle state as well as for the  $0_3^+$  and the  $2_2^+$  state. In the cluster models the absence of spin-orbit forces leads to the well known underestimation of the  $2_1^+$  energy indicating again their schematic nature.

To quantify the degree of  $\alpha$ -clustering within the FMD wave functions, which are obtained by a multiconfiguration mixing calculation containing shell-model like and cluster states, we calculate the overlap of the eigenstates with the  $\alpha$ -cluster model space. For that we construct a projection operator  $P_\alpha$  using the 165  $\alpha$ -cluster triangle configurations. We obtain  $\langle 0_1^+ | P_\alpha | 0_1^+ \rangle = 0.52$ ,  $\langle 0_2^+ | P_\alpha | 0_2^+ \rangle = 0.85$ ,  $\langle 0_3^+ | P_\alpha | 0_3^+ \rangle = 0.92$ ,  $\langle 2_1^+ | P_\alpha | 2_1^+ \rangle =$

TABLE I: Energies, radii and transition strengths. Units of energies are MeV, of radii fm,  $M(E0)$  efm<sup>2</sup>, and  $B(E2)$  e<sup>2</sup>fm<sup>4</sup>. Data are from [27], ‘BEC’ results from [12].

	Exp	FMD	$\alpha$ -cluster	‘BEC’
$E(0_1^+)$	-92.16	-92.64	-89.56	-89.52
$E^*(0_2^+)$	7.65	9.50	7.89	7.73
$E(0_2^+) - E(3\alpha)$	0.38	0.44	0.38	0.26
$E^*(0_3^+)$	(10.3)	11.90	10.33	
$E^*(2_1^+)$	4.44	5.31	2.56	2.81
$E^*(2_2^+)$	(11.16)	11.83	9.21	
$E(3\alpha)$	-84.89	-83.59	-82.05	-82.05
$r_{\text{charge}}(0_1^+)$	$2.47 \pm 0.02$	2.53	2.54	
$r(0_1^+)$		2.39	2.40	2.40
$r(0_2^+)$		3.38	3.71	3.83
$r(0_3^+)$		4.62	4.75	
$r(2_1^+)$		2.50	2.37	2.38
$r(2_2^+)$		4.43	4.02	
$M(E0, 0_1^+ \rightarrow 0_2^+)$	$5.4 \pm 0.2$	6.53	6.52	6.45
$B(E2, 2_1^+ \rightarrow 0_1^+)$	$7.6 \pm 0.4$	8.69	9.16	
$B(E2, 2_1^+ \rightarrow 0_2^+)$	$2.6 \pm 0.4$	3.83	0.84	

0.67 and  $\langle 2_2^+ | P_\alpha | 2_2^+ \rangle = 0.99$ . A restriction to  $\alpha$ -cluster configurations is obviously not sufficient for a description of the ground state. The spin-orbit force breaks the  $\alpha$ -clusters and a large shell-model component is found in the FMD ground state. The Hoyle state on the other hand is dominated by  $\alpha$ -cluster contributions but still has a sizable component of shell-model nature.

In Fig. 1, we compare calculated electron scattering form factors with measured data and show the corresponding charge densities for the ground state, the Hoyle state, and the transition between them. The data are given as the ratio of the measured cross section to the Mott cross section. The comparison between experimental and theoretical cross sections is performed in distorted wave Born approximation (DWBA) [29]. Although the transparent relation between form factors and charge densities as Fourier transforms of each other obtained in plane wave Born approximation (PWBA) is lost, it is preferred because the corrections are sizable, in particular at higher momentum transfers.

In the FMD and the  $\alpha$ -cluster model we calculate the densities of point-like protons and neutrons which are then folded with proton and neutron charge densities to obtain the densities shown in Fig. 1. The same proton and neutron charge densities are used to calculate the densities from the matter densities obtained within the ‘BEC’ model [16].

A good reproduction of the ground state form factor is a precondition to draw sound conclusions on the charge distribution of the Hoyle state from the transition form

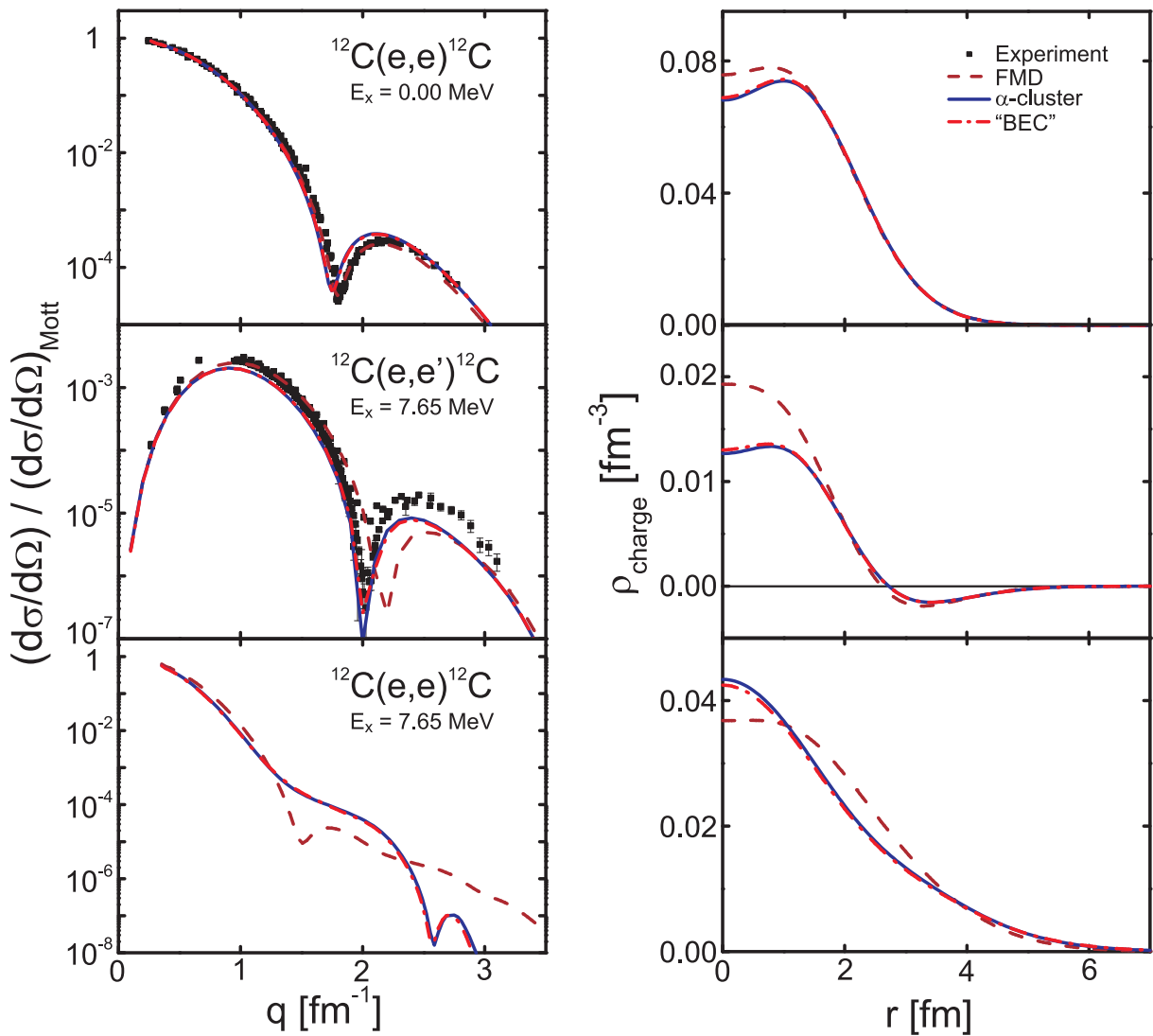


FIG. 1: (Color online) L.h.s.: FMD (dashed lines),  $\alpha$ -cluster (solid lines), and ‘BEC’ (dashed-dotted lines) predictions of the charge form factors in  $^{12}\text{C}$  in comparison to experimental data (full squares). Top: elastic scattering on g.s., middle: transition to the Hoyle state, r.h.s.: elastic scattering on the Hoyle state. R.h.s.: Corresponding charge density distributions. ‘BEC’ results are from [16].

factor because both states enter the transition matrix element on equal footing. As can be seen from Fig. 1 the ground state form factor is described well by the FMD model. The results for the  $\alpha$ -cluster and ‘BEC’ models are almost identical and show a slightly worse agreement with the data. Modifications by neglected contributions from meson exchange currents are expected to be small [30, 31].

The  $\alpha$ -cluster model and the ‘BEC’ very nicely reproduce the shape of the transition form factors but somewhat underestimate the magnitude of the form factors. The FMD model on the other hand gives a good description of the first maximum but has its node at  $q = 2.2\text{fm}^{-1}$  while the experimental minimum is at  $q = 2.0\text{fm}^{-1}$ . The differences in the transition form factors are mainly due

to differences in the Hoyle state. The FMD charge density of the Hoyle state has a smaller surface thickness and a lower central density, leading to a stronger oscillation in the transition density. These differences also show up in the form factors of the Hoyle state where the models show noticeable differences at medium and high momentum transfers. We suspect that minor modifications of the FMD interaction, taking  $\alpha$ - $\alpha$  scattering data into account, could result in an improved description – investigations are under way.

Charge densities and form factors are essentially one-body observables and do not reflect many-body correlations existing in the many-body state. Therefore the form factors provide no direct information on the  $\alpha$ -cluster structure, neither in the ground state nor in the Hoyle

state. However, as shown below a cluster nature of the Hoyle state is also supported by the FMD calculations, where the Hamiltonian can choose between shell-model like and cluster configurations. An analysis of the FMD Hoyle state shows that its leading components displayed in Fig. 2 are cluster-like and resemble  ${}^8\text{Be} + \alpha$  configurations. Two of the  $\alpha$  particles are typically close to each other and the third one is further away. The ground state is dominated by more compact configurations which have a large overlap with shell-model states (see r.h.s of Fig. 2). In the  $0_3^+$  and  $2_2^+$  states we also find the leading components to be of  ${}^8\text{Be} + \alpha$  nature but featuring more prolate open triangle configurations.

To summarize, high precision electron scattering data for elastic scattering and the transition to the Hoyle state at  $E^* = 7.654$  MeV with  $J^\pi = 0^+$  serve as an important test of the nature of the  $0^+$  states in  ${}^{12}\text{C}$ . The data are in accord with a Hoyle state that has low density, in the centre about half of that of the ground state, and a large spatial extension with a rms-radius that is about 1.5 times bigger than that of the ground state. These type of density profiles are predicted by Fermionic Molecular Dynamics and  $\alpha$ -cluster models. While the latter more schematic models presuppose the  $\alpha$ -structure, FMD does not but still predicts the Hoyle state to be dominantly composed of three weakly bound  $\alpha$  particles. The FMD calculations also show that the relative positions of the  $\alpha$ -clusters are correlated mostly resembling  ${}^8\text{Be}$  plus  $\alpha$  configurations. This correlation and the fact that anti-symmetrization is not negligible is in contradiction to a naïve interpretation of the ‘BEC’ wave function as a true Bose-Einstein condensate.

A final conclusion on the nature of the Hoyle state certainly requires further experimental and theoretical efforts. The model calculations should be extended to test further observables like decay features or scattering with hadronic probes. It might also be interesting to investigate the problem in other ‘ab initio’ approaches like the Green’s Function Monte Carlo method [32]. Finally, the Hoyle state could be a prototype for a whole class of such states near the  $\alpha$ -particle thresholds in light self-conjugate  $4n$  nuclei like in  ${}^{16}\text{O}$  [11] or even more exotic states [33]. Electron scattering will be an indispensable tool to resolve these questions and experimental studies of other candidate states are underway.

We are very much indebted to H. Crannell for providing us with many unpublished ( $e, e'$ ) data and to P. Schuck and Y. Funaki for the  $\alpha$ -cluster condensate model results. This work has been supported by the DFG under contract SFB 634.

- 
- [1] E. E. Salpeter, *Ap. J.* **115**, 326 (1952).
  - [2] F. Hoyle, *Ap. J. Suppl.* **1**, 121 (1954).
  - [3] C. W. Cook *et al.*, *Phys. Rev.* **107**, 508 (1957).
  - [4] S. M. Austin, *Nucl. Phys.* **A758**, 375c (2005).
  - [5] F. Herwig, S. M. Austin, and J. C. Lattanzio, *Phys. Rev. C* **73**, 025802 (2006).
  - [6] P. Navratil, J. P. Vary, and B. R. Barrett; *Phys. Rev. Lett.* **84**, 5728 (2000); J. P. Vary *et al.*, *Nucl. Phys.* **A746**, 123c (2004).
  - [7] H. Pichler *et al.*, *Nucl. Phys.* **A618**, 55 (1997).
  - [8] R. Bijker and F. Iachello, *Phys. Rev. C* **61**, 067305 (2000).
  - [9] P. Descouvemont, *Nucl. Phys.* **A709**, 275 (2002).
  - [10] S. I. Fedotov *et al.*, *Phys. Rev. C* **70**, 014006 (2004).
  - [11] A. Tohsaki *et al.*, *Phys. Rev. Lett.* **87**, 192501 (2001).
  - [12] Y. Funaki *et al.*, *Phys. Rev. C* **67**, 051306(R) (2003).
  - [13] T. Yamada and P. Schuck, *Phys. Rev. C* **69**, 024309 (2004).
  - [14] Y. Funaki *et al.*, *Eur. Phys. J. A* **24**, 321 (2005).
  - [15] T. Yamada and P. Schuck, *Eur. Phys. J. A* **26**, 185 (2005).
  - [16] Y. Funaki *et al.*, *Eur. Phys. J. A* **28**, 259 (2006); Y. Funaki, private communication.
  - [17] W. Reuter *et al.*, *Phys. Rev. C* **26**, 806 (1982).
  - [18] H. Crannell *et al.*, *Nucl. Phys.* **A758**, 399c (2005); H. Crannell, private communication.
  - [19] A. Lenhardt *et al.*, *Nucl. Instrum. Meth. Phys. Res. A* **562**, 320 (2006).
  - [20] P. Strehl, *Z. Phys.* **234**, 416 (1970).
  - [21] R. Roth, T. Neff, H. Hergert, and H. Feldmeier, *Nucl. Phys.* **A745**, 3 (2004).
  - [22] T. Neff, H. Feldmeier, *Nucl. Phys.* **A738**, 357 (2004); R. Roth *et al.*, *Phys. Rev. C* **72**, 034002 (2005).
  - [23] Y. Kanada-En’yo, *nucl-th/0605047*.
  - [24] D.M. Brink, *Proc. Intern. School Phys. ‘Enrico Fermi’ course XXXVI* (Academic Press, New York/London, 1966) p. 247.
  - [25] Y. Fukushima and M. Kamimura, *J. Phys. Soc. Japan Suppl.* **44**, 225 (1978); M. Kamimura, *Nucl. Phys.* **A351**, 456 (1981).
  - [26] H. Matsumara and Y. Suzuki, *Nucl. Phys.* **A739**, 238 (2004).
  - [27] F. Ajzenberg-Selove, *Nucl. Phys.* **A506**, 1 (1990).
  - [28] J. Friedrich and Th. Walcher, *Eur. Phys. J. A* **17**, 607 (2003).
  - [29] C. Bähr, code PHASHI, TU Darmstadt, unpublished; J. Heisenberg and H. P. Blok, *Annu. Rev. Nucl. Part. Sci.* **33**, 569 (1983).
  - [30] D. O. Riska, *Phys. Rep.* **181**, 207 (1989).
  - [31] A. M. Lallena, *Nucl. Phys.* **A615**, 325 (1997).
  - [32] S. C. Pieper and R. B. Wiringa, *Annu. Rev. Nucl. Part. Sci.* **51**, 53 (2001).
  - [33] Tz. Kokalova *et al.*, *Phys. Rev. Lett.* **96**, 192502 (2006).

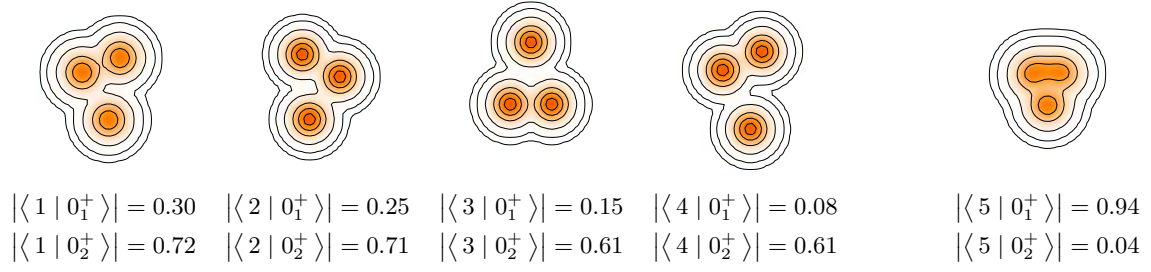


FIG. 2: (Color online) Intrinsic one-body densities of the four FMD states which contribute most to the Hoyle state and their respective amplitudes for the ground state ( $0_1^+$ ) and the Hoyle state ( $0_2^+$ ). The fifth state, obtained by variation after projection on angular momentum, is the leading component in the ground state. Note that the FMD states are not orthogonal.